Pergamon

Journal of Structural Geology, Vol. 18, No. 5, pp. 549 to 561, 1996

0191-8141/96 $15.00+0.00

0191-8141(95)00136-0

Progressive eclogitization under fluid-present conditions of pre-Alpine mafic granulites in the Austroalpine Mt Emilius Klippe (Italian Western Alps)

G. PENNACCHIONI

Dipartimento di Geologia, Paleontologia e Geofisica, via Giotto 1, 35137 Padova, Italy

(*Received* 6 *February* 1995; *accepted in revised form* 19 *October* 1995)

Abstract—Metabasites from the Austroalpine Mt Emilius Klippe preserve different stages of the evolution from pre-Alpine granulite- to Alpine eclogite-facies assemblages. The pre-Alpine protolith includes layered garnet I–clinopyroxene I–plagioclase–hornblende granulites and gabbros. The eclogitic paragenesis comprises garnet II–clinopyroxene II–epidote–Ca-amphibole ± chlorite. Eclogitic deformation is composite and involves two main episodes (D_{1A}, D_{1B}). D_{1A} produces a layer-parallel foliation and incomplete transformation of granulites and is concluded by an episode of brittle deformation leading to the formation of eclogitic veins. D_{1B} gives rise to widespread *S*–*L*-tectonites and mylonites. The eclogitic veins and surrounding haloes, enriched in fluids during veining, control the nucleation of D_{1B} shear zones. Deformation is accomplished through ductile flow of reaction-weakened plagioclase and hornblende sites and cataclasis of garnet I and clinopyroxene I. Both meso- and microscale observations indicate that fluids play a primary role during eclogitization in both enhancing deformation and the kinetics of metamorphic reactions. Fluids influence plastic flow rates in matrix aggregates and promote fracturing of hard minerals. The extent of metamorphic re-equilibration is closely related to the density of the fluid pathways. Copyright © 1996 Elsevier Science Ltd

INTRODUCTION

The study of rocks preserving a low-temperature eclogite-facies metamorphism offers the opportunity for gaining information on deformation mechanisms effective at depth in subduction zones. However, suitable sites for such a study are rare, as most eclogites are severely to completely overprinted by decompressional assemblages during exhumation. Moreover, eclogitization has often run to completion in well-preserved eclogitic sections, thus obscuring the reaction vs deformation pathways.

The metastable persistence of mineral relics in coarse-grained rocks along common pressure–temperature–time paths of Alpine eclogites is favoured by the slow volume diffusion rates in most silicates at the corresponding relatively low temperature ($T < 550$°C: see Droop *et al.* 1990, Dal Piaz *et al.* 1993 for a review and references therein). This tendency is counteracted by the catalytic effect exerted by strain-induced grain refinement processes and dislocation creep during ductile deformation on mineral reaction kinetics (Yund & Tullis 1980, Yund *et al.* 1981, Brodie & Rutter 1985). Heterogeneous strain distribution during polyphase metamorphism along a pressure–temperature–time path thus allows the observation of different stages of mineral evolution. The low-strain domains are the site of incomplete reactions, chemical disequilibrium and coronitic textures, and in these domains mineral relics are preserved. On the other hand, highly strained domains are preferential sites for pervasive metamorphic equilibration to synkinematic pressure–temperature conditions.

The development of strain gradients is often strongly dependent on the presence of primary rheologic heterogeneities. Metabasite pods embedded in micaschists and calcschists from both ocean- and continent-derived sheets are generally more resistant to deformation than the surrounding rocks along the whole pressure–temperature path. Thus, metabasites are capable of recording and preserving the different steps in the process of eclogitization, escaping both penetrative eclogitization and decompressional re-equilibration. However, field mapping often indicates that large volumes of metabasites have been converted to foliated eclogites even when the protolith is a coarse-grained rock. One reason for the enhanced ductility of metabasites under eclogitic conditions is the presence of fluids. A syneclogitic aqueous fluid phase has been well documented for several eclogite-facies rocks (e.g. Austrheim 1987, Philippot 1987). The effect of fluids may be multifold (Thompson & Rubie 1985, Rubie 1986), increasing the interface kinetics and rate of diffusion as well as producing hydrolytic weakening in silicates.

The complex interplay between fluids and deformation in the process of eclogitization is the topic of this work. The selected example is a body of metabasites from the Austroalpine Mt Emilius Klippe, where deformation partitioning during eclogite-facies conditions allows the progressive textural and mineral evolution to be followed from pre-Alpine medium-grained granulites to Alpine foliated eclogites.

GEOLOGICAL OUTLINE

The Mt Emilius Klippe (Italian Western Alps) is a continental basement unit of the Alpine nappe stack, cropping out south of the Aosta Valley on top of ophiolites of the Piemonte nappe (Fig. 1). It belongs to the

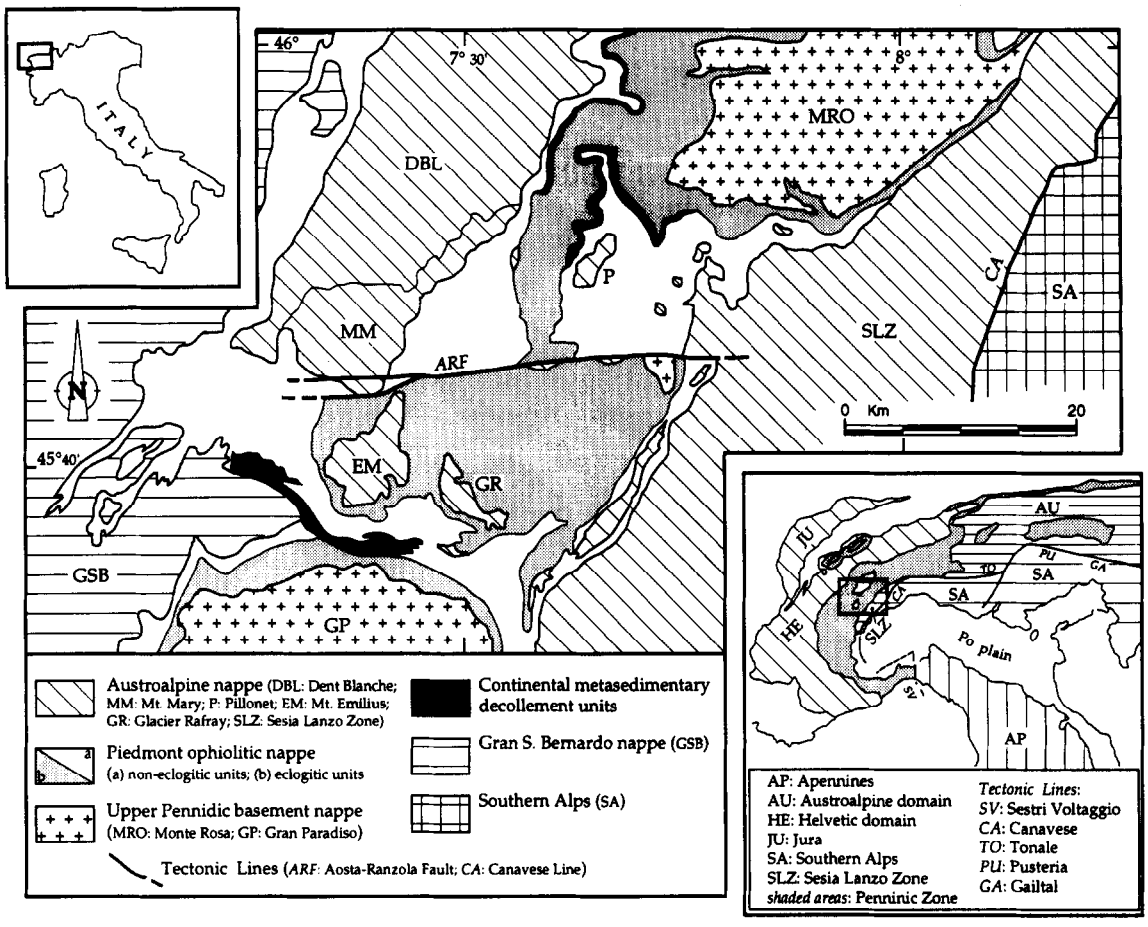

Fig. 1. Structural sketch map of the northwestern Alps.

lower element of the Austroalpine nappe (Ballèvre *et al.* 1986), a section of high-grade pre-Alpine continental crust referred to the Jurassic Adriatic plate margin and strongly involved in the Alpine orogenesis (Compagnoni *et al.* 1977).

Subduction-induced eclogite-facies assemblages of Cretaceous–Paleocene (eo-Alpine) age are well recorded in the Mt Emilius Klippe. The high-pressure assemblages are followed by a Mid-Tertiary (meso-Alpine) greenschist-facies overprint, acquired during the exhumation trajectory (Bearth *et al.* 1980, Dal Piaz *et al.* 1983). Temperatures of 450–550°C, with minimum pressures of 11–13 kbar, have been estimated for the high-pressure metamorphism (Dal Piaz *et al.* 1983, Pennacchioni 1991). The Alpine metamorphic evolution is accompanied by polyphase ductile deformation (D_1, D_2, D_3) (Dal Piaz *et al.* 1983, Pennacchioni 1991). D_1 and D_2 developed under high-pressure conditions; D_3 occurred during the greenschist-facies event. Owing to the heterogeneous character of deformation, relics of the different metamorphic and structural stages are preserved.

The pre-Alpine protoliths of the Mt Emilius rocks consist of granitoids and sillimanite–biotite–garnet–plagioclase-bearing paragneisses ('Kinzigites' *Auct.*), including quartz–plagioclase pegmatitic dykes and veins, pods and layers of mafic rocks, and calcsilicate marbles. They have generally undergone a penetrative metamorphic and structural reworking under eclogitic conditions, which has produced the main regional schistosity (S_1), and a later discontinuous greenschist-facies retrogression. The paragneisses have been largely converted under high-pressure conditions to garnet–glaucophane (±Na-clinopyroxene)-bearing phengitic micaschists and kyanite–chloritoid–garnet-bearing micaschist ('eclogitic micaschist complex' *Auct.*).

Inside the 'eclogitic micaschists' of the Mt Emilius Klippe, different types of metabasic rocks are distinguished on the basis of the high-pressure Alpine metamorphic assemblage (Pennacchioni 1991): (i) medium- to fine-grained omphacite + glaucophane + zoisite–clinozoisite + phengite + rutile–titanite-bearing eclogites often occurring in association with garnet glaucophanites and omphacitites; (ii) massive, relatively coarse-grained omphacite + garnet ± epidote ± titanite eclogites; and (iii) garnet + clinopyroxene + zoisite–clinozoisite + colourless amphibole (tremolite–actinolite)+ Mg-chlorite metabasites (glaucophane is always absent in such assemblages). The last lithotype is derived from pre-Alpine mafic granulites and is described in detail below.

ECLOGITIZED GRANULITES: FIELD DESCRIPTION

The main outcrop of eclogitized granulites is a huge body, exposed inside the eclogitic micaschists in the

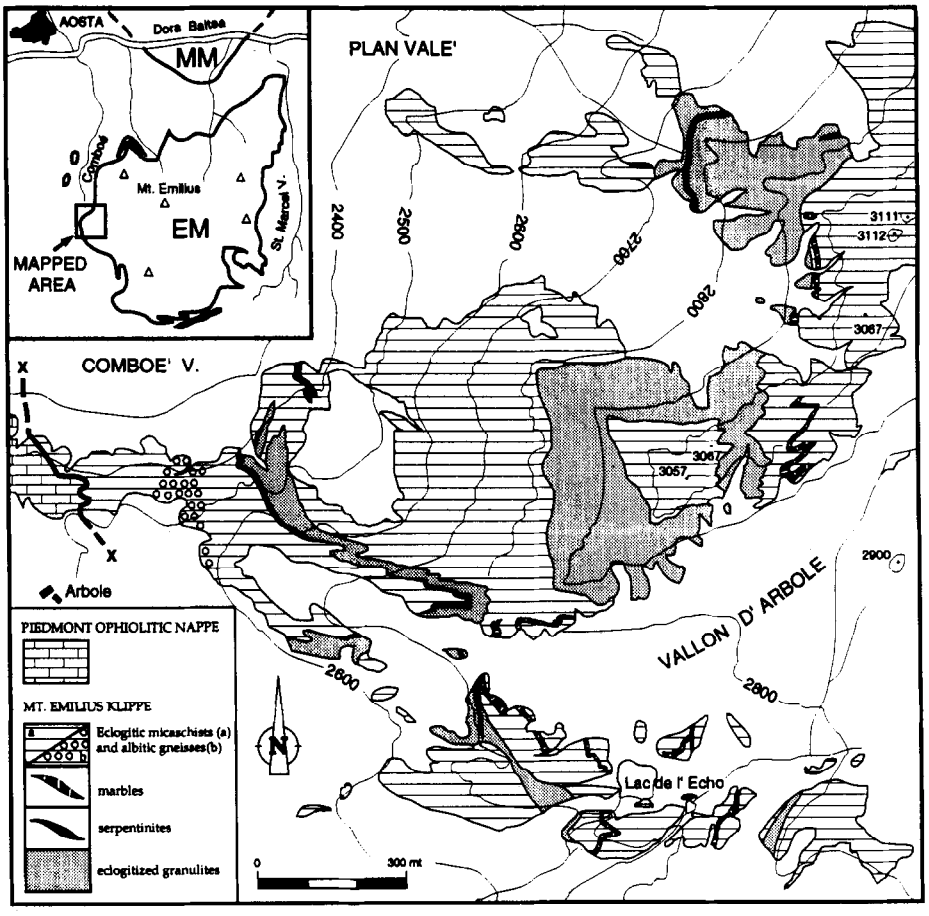

Fig. 2. Geological map of the Plan Valè-Arbole granulitic body. Locality names refer to the regional topographic sheets. Inset: Austroalpine Mt Mary (MM) and Mt Emilius Klippe (EM).

northwestern sector of the Mt Emilius Klippe (Fig. 2). Minor layers of serpentinite and silicate-bearing marbles are associated with metabasites in the body. The marbles contain pods (up to some metres thick) of massive coarse-grained garnet–diopside fels, which have been converted to fine-grained epidote–diopside–garnet mylonites during eclogitic deformation.

The mesoscopic deformation features recognized in the granulites are summarized in Fig. 3. The Alpine deformation history includes a composite eclogite-facies phase (D_{1A} and D_{1B}), which is responsible for the prominent foliations in the eclogitized granulites (S_{1A} and S_{1B}), and two main post-eclogitic folding phases (D_2 and D_3).

The distribution of D_{1B} deformation is heterogeneous. Most metabasites (>80%) have undergone strong mylonitic reworking during the D_{1B} deformation and only minor pods preserve relics of the pre-Alpine high-temperature protolith (Fig. 4a), more or less overprinted by the S_{1A} foliation. The occurrence of pre-Alpine mineral relics in the area was noted by Bearth *et al.* (1980) and by Benciolini (1989). In the low-strain domains, high-temperature mafic rocks display a cm- to m-scale layering (S_0), which includes: (i) medium-grained garnet–diopside–plagioclase–hornblende and diopside–plagioclase granulites; (ii) coarse-grained layers consisting of cm-sized black to deep violet clinopyroxene; and (iii) minor dykelets and m-thick discontinuous layers of clinopyroxene-bearing gabbros parallel to S_0. The granulitic layering is overprinted by a layer-parallel foliation and mylonites during D_{1A}.

In the (D_{1B}) low-strain domains, D_{1B} deformation is strongly localized in cm- to dm-thick ductile shear-zones (Fig. 4b) and interspersed mm-thick 'second-order' shear zones cutting across S_0 and S_{1A}. The shear zones are subparallel and, more rarely, anastomosing or conjugate and commonly accommodate very high shear strains ($\gamma > 10$), as estimated from the attitude of the shear zone foliation. The granulitic layering and S_{1A} foliation, bounded by subplanar D_{1B} shear zones in the low-strain domains, are often deformed by open to tight folds. The axial plane of folds parallels the shear plane S_{1B} and the fold axes parallel the mineral stretching lineation in the D_{1B} mylonites. These folds may develop synkinematically to D_{1B} deformation during partitioning of simple and pure shear components into high- and low-strain domains, respectively.

In the (D_{1B}) high-strain zones, metabasites have acquired a penetrative S–L-type tectonite fabric. Locally, highly stretched fabrics ($L > S$) to L-type fabrics predominate. Mineral stretching lineations are rather constant in orientation and trend around NNE–SSW (inset in Fig. 3).

Symmetric to asymmetric boudinage and schistosity boudinage are common and pressure shadows are filled with fibrous amphibole ± garnet. Boudinage occurs

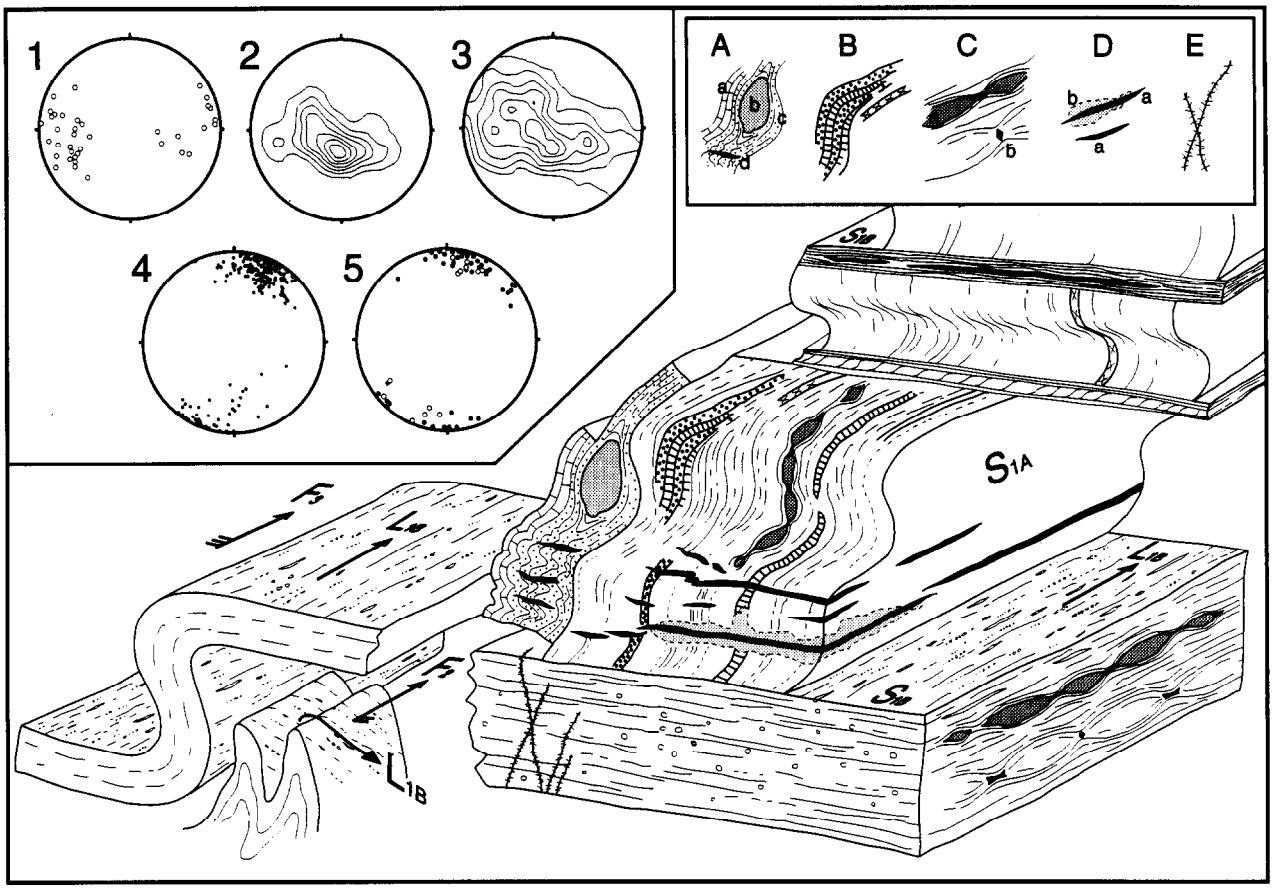

Fig. 3. Schematic block diagram summarizing the structural relationships between the mesoscopic fabric elements in metagranulites. (A) a—Marbles, b—garnet–diopside fels, c—garnet–diopside–epidote mylonites and d—diopside veins; (B) granulitic compositional layering (S_0); (C) a—boudinage and b—schistosity boudinage with amphibole±garnet-filled pressure shadows; (D) a—syneclogitic veins and b—omphacitization haloes; (E) late amphibole-filled veins. Orientation data are shown in the equal area, lower-hemisphere stereographic projections in the upper-left corner inset: (1) S_{1A} in granulites (40 data); (2) S_{1B} in granulites (384 data; contouring at 1, 2, 3 . . . times uniform); (3) S_{1B} in micaschist (979 data; contouring at 0.5, 1, 1.5 . . . times uniform); (4) mineral stretching lineation L_{1B} (170 data); (5) fold axis: F_3 (filled circles; 47 data) and F_2 (open circles; 15 data).

along both S_{1A} and S_{1B}. Boudin orientation in S_{1B} indicates a maximum extension direction parallel to the mineral stretching lineation of the tectonites.

Mineral veins

The presence of fluids during the high-pressure stage is recorded in the field by the common occurrence of veins with eclogite-facies mineral infilling. High-pressure veins cut, at high angles, across S_{1A} and the high-temperature layering, and are frequently associated with D_{1B} shear zones and folds, developing parallel to the shear plane or to the axial plane of folds (Figs. 4c–e). The veins have different mineralogy and include garnet, epidote, clinopyroxene and amphibole. A common type is a mm-thick epidote-rich–garnet–clinopyroxene vein (Fig. 4f). Garnet typically develops as small crystals at the vein selvages. Clinopyroxene-rich veins (Fig. 4g) have thicknesses up to some centimetres and garnet walls are absent. Veins include garnet and clinopyroxene–epidote in clinopyroxene layers, and diopside in epidote–diopside–garnet mylonites associated with marbles.

The veins are generally parallel-sided and persistent over distances of several decimetres to metres, and occur as parallel or, locally, conjugate sets. Thick clinopyroxene veins are sometimes found as en echelon sigmoidal-shaped sets.

In metabasites, light green haloes rich in omphacite border some clinopyroxene veins (Fig. 4h). In the thickest veins, haloes of omphacite are up to 10 cm thick. Omphacitization clearly overprints the S_{1A} fabric. Similar examples of 'eclogitization' of granulites around shear zones and veins have been described, for instance, in granulite-facies anorthosites of the Bergen arc, Western Norway (Austrheim 1987, Boundy *et al.* 1992).

High-pressure veins are normally sheared parallel to the vein walls and to the shear foliation during D_{1B} deformation. Therefore, the veins either pre-date the shear zone development or have originated synkinematically as shear veins and have rotated into parallelism with shear plane during progressive deformation. The first assumption is strongly supported by the fact that shear deformation is sometimes limited to the veins and that undeformed or slightly deformed veins occur, in the low-strain domains, parallel to the shear zones. The veins probably originated as tensile and shear fractures during the final stages of S_{1A} formation.

Other veins in the eclogitized granulites probably post-dated the eclogitic metamorphism. They form sub-parallel sets of thin amphibole-filled fractures cross-cutting the S_{1B} foliation.

Post-mylonitic ductile deformations

The eclogitic mylonites and tectonites are deformed by D_2 and D_3 folds. D_{3+2} overprinting patterns are of type III of Ramsay (1967). Fold axes assigned to D_2 and D_3 are plotted in the stereograms of Fig. 3. In some rare cases, the mylonitic lineation is seen to cross-cut D_2 fold hinges. In contrast, the lineation is always parallel to the D_3 fold axis. This could be related to the strong linear anisotropy of the mylonites and tectonites controlling the nucleation of D_3 folds (Watkinson & Cobbold 1981). At the scale of hundreds of metres, the D_3 deformation produces asymmetric S-shaped folds looking north.

MICROSTRUCTURAL ANALYSIS

Different kinds of microstructural domains can be distinguished.

(a) *Low-strain domains* retain good overall textural and mineral evidence of the pre-Alpine high-temperature metamorphic stage, but totally unreacted domains do not occur. At the thin section scale, even in the best preserved samples, deformation is related to a network of microshear zones and microfractures.

(b) *Foliated* (S_{1A}) *metagranulites* are weakly to moderately strained rocks, closely associated with undeformed granulites, which preserve widespread mineral relics of clinopyroxene I and garnet I. The development of the foliation, defined by elongation of plagioclase and hornblende pseudomorphs, is not accompanied by the extensive amphibole-filled pressure-shadowing around porphyroclasts that characterizes the mylonites.

(c) *Mylonites* show a well-developed lineation and/or foliation. A typical mm-banding develops by deformation of the fine-grained aggregates, derived from the breakdown of plagioclase and hornblende, and by metamorphic differentiation. Small porphyroclasts of garnet I and clinopyroxene I are common inside the fine-grained matrix, but are often extensively replaced.

(d) *Ultramylonites* are very fine-grained rocks where complete metamorphic recrystallization and fabric reconstruction occur.

Low-strain domains and foliated metagranulites

The high-temperature mineralogy and microstructure preserved in the low-strain domains allow the relic fabric to be assigned to the pre-Alpine metamorphism. The high-temperature minerals are no longer stable under the new metamorphic conditions. However, porphyroblastic garnet I and clinopyroxene I occur as widespread mineral relics. The other high-temperature minerals are inferred to be Ca-rich plagioclase and hornblende from their breakdown products.

Garnet. In granulites, two generations of garnet (garnet I, garnet II) are identified. Porphyroblastic pre-Alpine garnet I, up to a few centimetres in size, has a typical high-temperature shape characterized by low-interfacial energy, coarse inclusions of clinopyroxene I, former plagioclase and hornblende (Fig. 5a). It shows coronas and bands, along cross-cutting microshear zones, of small (10–100 μm) garnet II idioblasts, rich in very fine-grained inclusions of epidote, amphibole and rutile, and displays a cataclastic texture sealed by garnet II, as evidenced by SEM (backscattered electron microscope) imaging (Fig. 5b), and by chlorite. The bands of garnet II, developed along fractures, range in thickness from a few to several tens of microns and interference between adjacent fractures commonly results in pervasive replacement of garnet I by garnet II. Fractures, which are often outlined by fluid inclusion trails, are randomly oriented and therefore suggestive of hydrofracturing, or are preferentially arrayed parallel to, or at high angle to, the foliation. The garnet I remnants, isolated by the network of microfractures filled by garnet II, are sometimes partly to completely replaced by Mg-chlorite or by chlorite ± epidote ± albite, and complete replacement of pre-Alpine garnet I cores produces atoll-like textures rimmed by garnet II. Chlorite displays sharp grain contacts with (coexisting) garnet II idioblasts.

Clinopyroxene. Pre-Alpine clinopyroxene I is clear, light-brown coloured salite. The clinopyroxene I commonly displays deformation features such as microfracturing, bending and ubiquitous undulatory extinction, and is progressively replaced, along grain boundaries and microfractures, by very fine-grained symplectites, colourless and green amphibole, garnet II, light-green clinopyroxene II, and by more rare chlorite and phengite. Different generations of microfractures can be distinguished (Figs. 5c & d). Early hornblende–chlorite lamellae, along cleavage planes of the clinopyroxene I, are overprinted by high-pressure microfractures occurring in parallel sets at high angles to the foliation. The high-pressure microfractures include fine-grained idioblastic garnet II and are surrounded by an irregular, discontinuous border of clinopyroxene II epitaxially overgrowing the clinopyroxene I. Idioblasts of colourless amphibole nucleate along hornblende–chlorite lamellae, garnet II-decorated microfractures and grain boundaries or grow scattered throughout the clinopyroxene I.

In clinopyroxene layers, garnet II occurs both as a blocky framework along the grain boundaries between centimetric clinopyroxene I and as small idioblasts along planar intracrystalline microfractures controlled by crystallographic directions (Fig. 5e). A narrow clear rim of epitaxial or fibrous clinopyroxene II is formed along garnet-decorated microfractures. Thicker isolated veins of blocky garnet II, fibrous clinopyroxene II and epidote cut across the whole coarse-grained aggregate. In clinopyroxene layers, strain increase resulted in breccia-like textures; clinopyroxene I fragments were displaced along the pervasive network of fractures and opening

voids were occupied by coarse clinopyroxene II ± amphibole fibres.

Plagioclase. Plagioclase is completely replaced by fine-grained aggregates of epidote (clinozoisite ± zoisite) with minor amounts of omphacite + amphibole ± quartz, even in undeformed sites. In low-strain domains, the plagioclase pseudomorphs are comprised of small irregular porphyroblasts of zoisite, showing intense intracrystalline deformation, and prismatic epidote often arranged in spray and garben-like or herring-bone arrays. Deformed aggregates of epidote mostly include equant to slightly elongated crystals, with strong preferred alignment. Grain boundaries are straight, sometimes defining polygonal textures, to slightly curved; larger crystals are frequently polygonized with low-mismatched 'subgrains'.

Hornblende. Hornblende, like plagioclase, is completely altered to aggregates of minerals with a dusty appearance under the microscope (Fig. 5f) owing to the presence of very fine-grained rutile. These aggregates consist of chlorite, garnet II, amphibole, epidote ± phengite. Garnet II occurs as small scattered idioblasts either arranged in rows along microfractures or as incomplete reaction coronas at the contact with the former plagioclase. The Ti-bearing mineral phases in these rocks are either titanite or rutile. Granoblastic aggregates of rutile are locally surrounded by coronas of garnet II.

Low-D_{1B} strain domains commonly show some minor reactivation of the fabric during the D_{1B} deformation. In foliated granulites, deformed pseudomorphs after plagioclase, elongated along S_{1A}, develop an internal transverse preferred shape orientation of epidote grains parallel to the S_{1B} foliation in the shear zones. In these rocks, most of amphibole growth is related to the D_{1B} overprint. Amphibole occurs in pressure shadows, discordant to the S_{1A} foliation, developed around clinopyroxene I porphyroclasts, and in microfractures of clinopyroxene I, reactivated during D_{1B} deformation or newly formed. Amphibole, similar to epidote, has a preferred shape orientation parallel to S_{1B}.

Mylonites and ultramylonites

Since D_{1A} and D_{1B} mylonites show similar microstructures and develop under similar metamorphic conditions they will be treated together.

In mylonites and ultramylonites, the foliation is defined by the preferred orientation of matrix epidote, amphibole, clinopyroxene and chlorite, and by a millimetric compositional layering, which was derived from deformation of mineral aggregates replacing the primary mineral sites and from metamorphic differentiation. Epidote-rich (mainly clinozoisite) layers were produced by stretching and coalescence of pseudomorphs after plagioclase. Ribbons of amphibole, epidote and chlorite represent the deformed pseudomorphs after hornblende, as is still suggested, in some cases, by the presence of a characteristic clouding. Clinopyroxene II occurs in bands of very fine-grained dynamically recrystallized aggregates (± amphibole and epidote), derived from clinopyroxene I, or in fibrous pressure shadows around garnet and clinopyroxene porphyroclasts. Elongated domains of amphibole, either strongly or randomly oriented, form pressure shadows around garnet porphyroclasts and are converted, with increasing strain and recrystallization of garnet, to amphibole-garnet II layers. Trails of titanite grains, which locally retain rutile cores, mark the foliation.

Relics of garnet I and clinopyroxene I commonly occur in the mylonites wrapped around by the foliation. Garnet I shows thick coronas of garnet II, rich in inclusions of titanite, rutile, epidote and amphibole, and is replaced, more or less extensively, by either chlorite or chlorite+albite+epidote aggregates. It is dismembered during deformation into irregular fragments, which are mostly recrystallized to framboidal aggregates of garnet II. Pressure shadows are filled with amphibole, clinopyroxene II and chlorite. In mylonites, garnet II has an average grain-size coarser than in granulites.

Clinopyroxene I porphyroclasts are completely replaced by epitaxial clinopyroxene II, or by an optically dusty fine-grained intergrowth of epitaxial clinopyroxene II and amphibole. Symplectitic aggregates are in turn overgrown by large randomly oriented amphibole idioblasts. The porphyroclasts are crowded with very fine grains of titanite, epidote and garnet II, which are often arranged as subparallel trails along high-angle microfractures. These substitutions are accompanied by grain-size reduction of clinopyroxene. Dusty relics of clinopyroxene I are displaced along microfractures and opening spaces are filled with colourless amphibole and clinopyroxene II fibres. In some cases, an optically clear epitaxial overgrowth of omphacite borders the porphyroblastic dusty cores at the pressure shadow interfaces.

Mylonites underwent post-kinematic static annealing, which resulted in a random, decussate fabric of amphibole aggregates, with grain-size coarsening and neocrystallization. The decompressional overprint is commonly recorded by static overgrowth of epitaxial rims of green-emerald amphibole around the colourless amphibole. In the same mylonites, clinopyroxene II is usually replaced along grain boundaries by the typical breakdown symplectites of very fine-grained diopside+albite and amphibole+albite, and the cores of garnet I, altered to chlorite, are replaced by chlorite + albite + Fe-epidote.

High-pressure veins

Weakly deformed veins are quite rare. Veins are commonly sheared parallel to the vein wall and the primary vein minerals are sometimes preserved as lenticular domains or bands surrounded by a fine-grained dynamically recrystallized matrix. Two main types of veins are recognized.

(1) Type-1 veins mainly consist of epidote. Infilling prismatic minerals (epidote, clinopyroxene) are roughly oriented with their long axis ([001] direction) approximately perpendicular to the vein wall or have a random orientation. Deformation was preferentially concen-

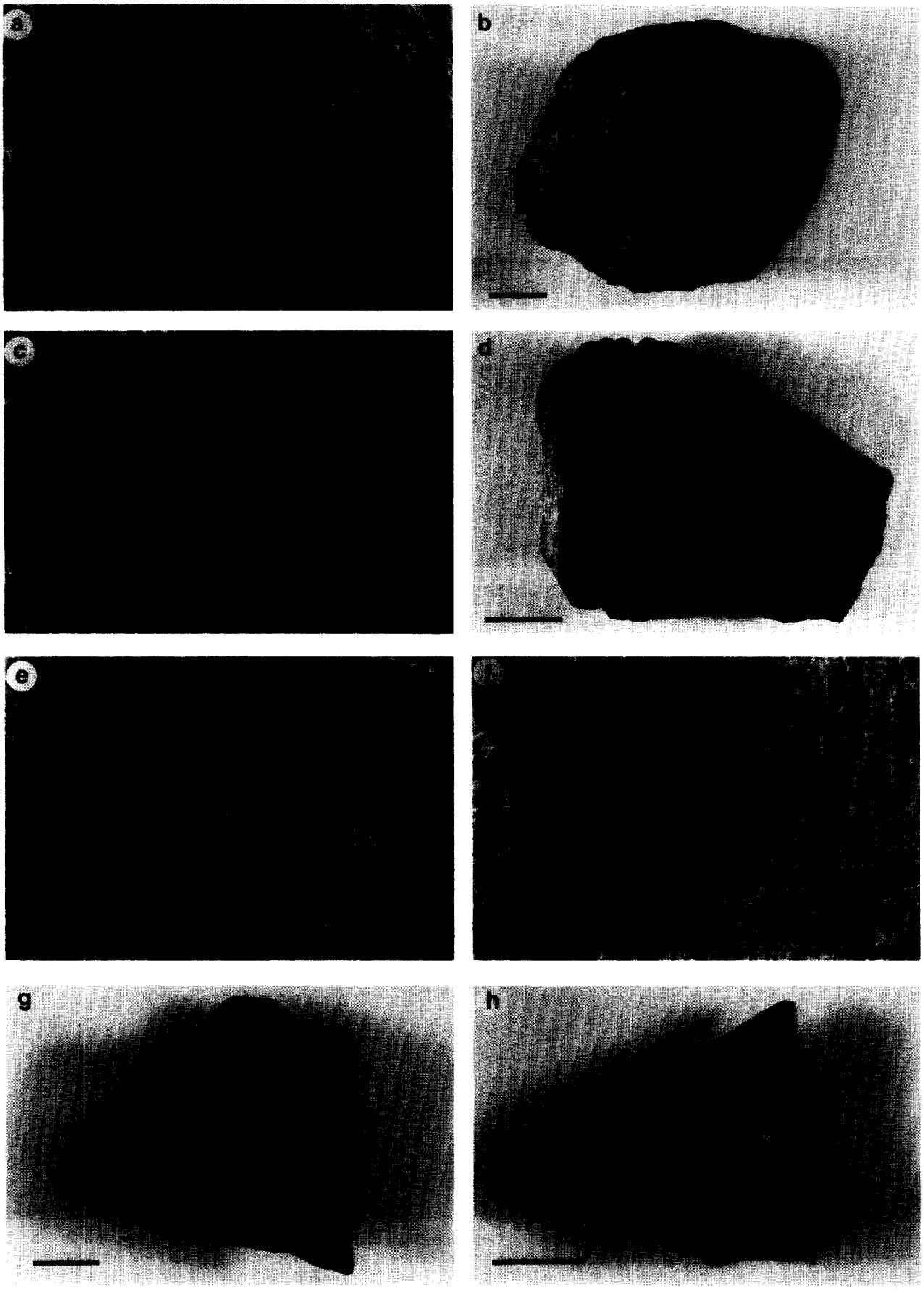

Fig. 4. Eclogite-facies shear zones and veins in the granulites. (a) Granulitic layering cut discordantly by D_{1B} mylonites; (b) narrow D_{1B} ultramylonite band cutting across slightly foliated granulites in (D_{1B}) low-strain areas; (c) epidote-rich vein occurring along the median line of a D_{1B} shear zone in granulites; (d) paired shear zones bordering an epidote–garnet vein; (e) sheared clinopyroxene veins (arrows) parallel to the axial plane of tight folds in layered granulites; (f) subparallel mm-thick epidote-rich veins in undeformed granulites. The thin darker walls are made of minute garnet II; (g) clinopyroxene and zoned clinopyroxene–epidote veins paralleling the axial plane of kink-like folds of the granulitic layering; (h) omphacite-rich halo (white arrow) around clinopyroxene–epidote vein (black arrow) cutting S_{1A} foliation. Scale bars (a, d, g & h) and diameter of the coin (b) are 2.5 cm. The pencil (c, e & f) is 15 cm long.

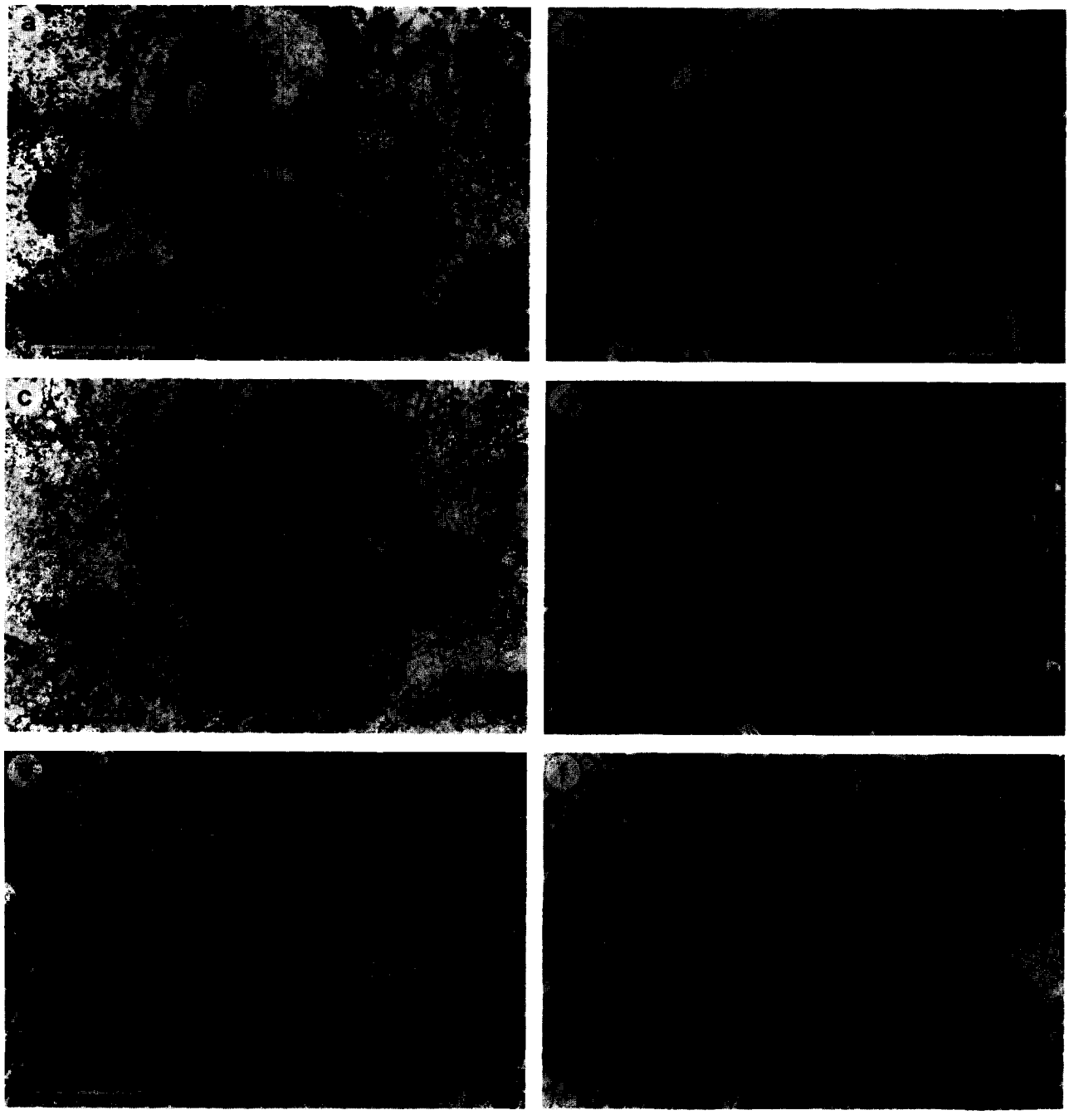

Fig. 5. Microstructures in the low-strain domains. (a) Granulitic garnet I porphyroblast with coarse inclusions of ovoid clinopyroxene I. Small pull-aparts along fractures (arrows) are occupied by clinopyroxene II and amphibole oriented parallel to the S_{1B} microshear zone in the lower part of the picture. Garnet I recrystallizes to fine-grained garnet II along the microshear zone. Scale bar is 2 mm. (b) Pervasive pattern of garnet II-healed microfractures (light bands) inside garnet I core in SEM backscatter image. Scale bar is 10 μm. (c) Relic clinopyroxene (Cpx I) with extensive sets of microfractures. Hornblende–chlorite lamellae (E–W-oriented dark bands) are cross-cut by high-pressure microfractures (NNW- and NNE-oriented) filled by garnet II, clinopyroxene II and amphibole, or outlined by dusty symplectites. Scale bar is 1 mm. (d) SEM backscatter image of microfractures in clinopyroxene (Cpx I). Amph: amphibole; CpxII: clinopyroxene II; Hbl–Chl: hornblende–chlorite lamellae; Grt II: garnet II (note the cataclastic internal texture). Scale bar is 100 μm. (e) Garnet II along cleavage-related microfractures in coarse-grained clinopyroxene layers; the narrow light border along the fractures is clinopyroxene II. Scale bar is 4 mm. (f) Fully replaced hornblende (Hbl) (sooty dusty domains) and plagioclase (Pl) (clear domains) sites coexisting with relic garnet I (Grt I) and clinopyroxene I (Cpx I) in nearly undeformed granulite. Scale bar is 1 mm.

trated in clinopyroxene, which is commonly recrystallized. Epidote is locally idioblastic and displays concentric and (rare) sector zoning. Near the vein walls, it often includes sheaves of amphibole needles. These features are consistent with crystallization into an open fluid-filled cavity (Durney & Ramsay 1973). A rough preferential orientation perpendicular to the vein wall may be owing to face-controlled growth at the vein wall and/or competitive growth between adjacent crystals. In garnet-bearing veins, garnet is always localized at the vein wall as single rows or bands of small idioblasts. Usually, garnet overlaps the wall rock–vein interface and shows a portion rich in inclusions on the side overgrowing the country rock, as opposed to a clear and inclusion-poor portion on the vein side. In cases in which the walls are sheared parallel to the vein, the inclusions in garnet are oriented and continuous with the external foliation. Garnet walls are assumed to have formed during a late stage of vein formation by reactivation of the vein–wall rock discontinuity.

(2) Type-2 veins comprise mainly clinopyroxene-rich veins and are characterized by a strong preferred orientation of the long axis of infilling prismatic minerals, which are arranged perpendicular to the walls. Fibres (shape elongation $\neq$ [001] direction) are rarely developed in the clinopyroxene and more commonly in epidote. Rare clinopyroxene fibres are observed as epitaxial overgrowth on clinopyroxene I of the vein wall, whereas epidote fibres nucleate on epidote domains of the wall rock. In contrast with type-1 veins, these veins are suggestive of a crack–seal type mechanism (Ramsay 1980, Philippot 1987), which results from progressive discrete periods of opening and healing of the fracture under deviatoric stress.

Both clinopyroxene and epidote contain abundant primary to pseudosecondary fluid inclusions of aqueous brines (Pennacchioni *et al.* 1993). In clinopyroxene, fluid inclusions generally show a tubular shape and are arranged, parallel to the clinopyroxene *c*-axis, in core clusters or along microfractures. Trails of fluid inclusions subparallel to the vein wall have been noted in epidote in type-1 veins.

STABILITY OF AMPHIBOLE AND CHLORITE DURING DEFORMATION

The high-pressure conditions of deformation in both the mylonites and the low-strain domains are clearly indicated by recrystallization and growth of clinopyroxene II and garnet II. The conditions of the eclogite-facies metamorphism have been estimated in the range of T = 450–550°C with minimum pressures of 11–13 kbar, on the basis of Fe–Mg partitioning between coexisting garnet–clinopyroxene and the jadeite content of the clinopyroxene, respectively (Dal Piaz *et al.* 1983, Pennacchioni 1991).

The main problem in the interpretation of the deformation fabrics during development of S_{1A} and S_{1B} is whether microstructures formed largely synkinematically with the eclogite-facies event, or are the result of superimposed post-eclogitic deformation and/or metamorphism. The question is not trivial, due to the occurrence of Ca-amphibole and chlorite along the clinopyroxene II–garnet II-bearing foliations, which is unusual in eclogite-facies assemblages. Bearth *et al.* (1980) interpreted the colourless amphibole in metabasics as a pre-eclogitic relic probably related to the prograde subduction path. This interpretation derives from the observation that glaucophane is the stable amphibole in most eclogites of the Mt Emilius Klippe and that the decompressional overprint gives rise to crystallization of amphiboles coexisting with albite. However, the absence of glaucophane in granulites and the presence of amphibole is better explained by differences in bulk chemical compositions of Mt Emilius mafic protoliths, as Na-amphibole does not nucleate at any time throughout the whole metamorphic history.

In granulites, amphibole occurs both along S_{1A} and S_{1B} mylonitic foliations, which also show dynamic recrystallization and growth of clinopyroxene II and garnet II. Shape preferred orientation of amphibole, chlorite and clinopyroxene II in matrix aggregates, grain-scale cracks and pressure shadows infilling combine to define the planar and linear-planar fabrics. Moreover, amphibole (±garnet) pressure shadows occur around boudins along both S_{1A} and S_{1B}. It must be remarked that the L_{1B} mineral stretching lineation in granulites, which is largely outlined by amphibole aggregates, parallels the lineation of fine-grained dynamically recrystallized omphacite-garnet eclogites inside the wall micaschists. All the observations point to a syneclogitic growth of both amphibole and chlorite. An alternative explanation could be that the S–L_{1B} fabric developed during 'coaxial' progressive deformation under metamorphic conditions changing from the omphacite to the plagioclase stability field. In this view, amphibole and chlorite belong to the post-eclogitic stage. This would imply a strong layer-parallel mylonitic reactivation of (amphibole-chlorite bearing) S_{1A}, which is very unlikely where S_{1A} is orthogonal to S_{1B}.

DISCUSSION

The development of an epidote–amphibole–chlorite ± phengite-bearing assemblage from a relatively anhydrous granulite-facies assemblage implies the introduction of an aqueous fluid phase into metabasites. The main episode of fluid infiltration probably predates the eclogite-facies ductile deformation. In fact, D_{1A} ductile deformation is mainly promoted by flow of plagioclase sites, which transform to fine-grained aggregates. A pre-eclogitic and/or pre-kinematic (static) pervasive transformation of plagioclase is suggested by the completeness of the transformation, independent of D_{1A} strain gradients. The occurrence of omphacite in the pseudomorphs after plagioclase points to a high-pressure transformation. The source for aqueous fluids

during high-pressure metamorphism may be dehydration reactions occurring in the eclogitic micaschists surrounding the metabasites, as demonstrated by Hy (1984) in the Sesia-Lanzo zone. Further fluid supply to the metabasites is possibly related to the veining episode concluding D_{1A} ductile deformation.

Some hydration may have occurred during the pre-eclogitic (pre-Alpine?) history of the metabasites, as it is supported by the occurrence of chlorite+hornblende lamellae in the clinopyroxene I. A pre-Alpine retrogression of the high-grade Mt Emilius protoliths, before the Alpine eclogite-facies overprint, is recorded in the Arpisson ultramafites (Benciolini 1989). Moreover, pre-eclogitic uplift has been recognized for various pre-Alpine high-grade units of the Western Alps (see review in Dal Piaz 1993).

Ductile–brittle transition during D_{1A}

The microscale deformation features indicate that deformation is largely accomplished by flow of the fine-grained mineral aggregates after plagioclase, which constitute the strain-supporting framework in metabasites. This suggests a grain-size-sensitive deformation mechanism. Thus, the transformation of plagioclase is critical for the onset of ductile behaviour of granulites during eclogite-facies conditions. Reaction-weakening producing a change in deformation mechanism, as a result of the transition from coarse- to fine-grained mineral aggregates, is well documented (e.g. Rubie 1983, Stünitz & Fitz Gerald 1993).

Deformation mechanisms are difficult to establish unambiguously on the basis of microstructural observations. However, the strong preferred alignment of grain boundaries and common planar grain contacts of fine-grained epidote-rich aggregates after plagioclase could be indicative of a process of viscous grain boundary sliding (Stünitz & Fitz Gerald 1993). The stability of deformation may be assured by inhibited grain growth due to the presence of minor amounts of clinopyroxene II, quartz and amphibole in the epidote aggregates and/or by dynamic recrystallization. Subgrain polygonization and recrystallization in large individuals of epidote may intervene when dimensions locally exceed the stable flow grain-size.

Fluid availability strongly controls the rate of deformation of the fine-grained aggregates after plagioclase. Steady-state viscous grain boundary sliding requires either dissolution–precipitation processes or diffusive and/or plastic material transfer as an accommodating mechanism (Gifkins 1976, McClay 1977). Besides influencing dissolution–precipitation, pore fluids facilitate diffusive mass transfer (White 1976) and increase the probability of the emergence of dislocations at grain boundaries, thus reducing the work-hardening that results from dislocation pile-up at crystal interfaces (Rutter 1972 and references therein). The dependence on fluids of deformability in the fine-grained aggregates is clearly evident during D_{1B} flow partitioning around veins (see later). Thus, the reaction softening effect, due to decrease in the grain-size, is reduced when hydration reactions are involved.

In mylonites, the presence of excess water during D_{1A} is unambiguously indicated by the widespread synkinematic growth of hydrated minerals and by fluid-assisted microfracturing of garnet I and clinopyroxene I. However, progressive lowering in the amount of free-fluids can occur during D_{1A}, by concurrent H_2O-consuming reactions (e.g. synkinematic replacement of clinopyroxene by amphibole), and result in strain hardening and final fracturing. This may explain the veining episode following D_{1A} ductile deformation.

In this interpretation, the re-establishment of ductile conditions during D_{1B} implies the renewed introduction of H_2O. Hydration is triggered by the same strain-hardening process that induces fracturing and the consequent recharge of fluids. Fluid infiltration occurs primarily by advection along vein sets, which allows rapid transport of fluids inside the granulites, and away from the veins by migration along grain-scale pathways such as grain boundaries and microcracks.

A geometric hardening effect (White *et al.* 1980, Shea & Kronenberg 1993), owing to the relative rotation of S_{1A} to an unfavourable orientation with respect to the stress axes, may have occurred concurrent with hardening related to the decrease in fluid availability. This process is corroborated by the orientation data for mesoscopic fabrics. If the contribution of geometric hardening is predominant, an external fluid influx is not necessary to restore ductile deformation; fluid infilling of the fractures may derive predominantly by drainage, from mylonites, of the residual pore fluids, moving under the pressure gradients induced by opening of the veins (the 'fluid pumping'-type mechanism of Sibson 1981). Flow of a saturated fluid towards the fracture assists solute transport. In the case of vein infilling indicative of crystallization in a open fluid-filled cavity, a local high wall-rock porosity reflecting high connectivity of fluid migration pathways is required to ensure rapid fluid influx and to keep the fracture open. Very well oriented vein infilling is best explained by an incremental history of vein opening (crack–seal mechanism) and implies lower rock permeabilities. After levelling of pressure gradients by fluid flow, an additional mass transfer component may be achieved by diffusive migration of solute under chemical potential gradients through a static intergranular fluid film (Philippot & Van Roermund 1992). Low fluid/rock and/or recycling of internal fluid instead of influx from outside micaschists during this veining episode is supported by the fact that compositions of vein filling minerals are strongly rock-buffered.

Fluid-induced deformation partitioning of D_{1B}

It is generally accepted that a mechanism of material strain softening, or loss of load-bearing capacity, is fundamental for localization of deformation. A number of softening mechanisms have been proposed, including

crystallographic preferred orientation softening, recrystallization softening, phase-change softening, fluid weakening and thermal softening (White *et al.* 1980). Most of these mechanisms are activated after the formation of a shear zone and allow further deformation to accentuate a pre-existing high-strain band, but they do not explain shear zone nucleation. Nucleation and localization are the two basic processes that produce partitioning of deformation. In the current case, there is strong evidence that nucleation of the shear zones and focusing of D_{1B} deformation is, at least in part, owing to the uneven distribution of aqueous fluids related to a precursor brittle episode. The process of fluid-induced nucleation and softening is demonstrated by the systematic occurrence of veins associated with shear zones and mylonites. The occurrence of deformation partitioning in rocks that have undergone a severe grain-size reduction clearly demonstrates the critical role of fluids on the flow properties of fine-grained rocks.

The formation of the veins as a precursor to the D_{1B} deformation has a double effect on the distribution of high-strain zones: (i) by inducing vein-related hydration gradients in the country rock close to the vein; and (ii) by creating planar discontinuities due to the different composition of the vein relative to the surrounding granulite (a geometric effect).

The anisotropy introduced by the vein–halo system influences the nucleation and successive growth of the related shear zones in two different ways, depending on the rheological contrast with the surrounding host rock.

(i) Epidote-rich veins with massive garnet–epidote walls act as strong domains with respect to granulites. This induces a perturbation in the stress field allowing high-strain deformation to concentrate on both sides of the vein system as well illustrated for flow around rigid rectangular objects (Ildefonse & Mancktelow 1993, Van Den Driessche & Brun 1987) and adjacent to stiff veins in rocks and glaciers (Hudleston 1989). The presence of hydration gradients in the country rock in the vicinity of the veins probably enhances ductility. The resulting structure consists of paired shear zones of the type shown in Fig. 4(d). Früh-Green (1994) suggests an analogous process ('fluid-induced reaction hardening') for the development of eclogite-facies mylonites in the metagranitoids of Mt Mucrone (Sesia Lanzo Zone).

(ii) In contrast, clinopyroxene-rich veins behave as softer zones and deformation concentrates within the vein. In most cases, clinopyroxene veins form strongly sheared zones inside undeformed or slightly deformed wall rocks. The crystal–plastic deformation of omphacite is well documented in eclogites (Buatier *et al.* 1991, Boundy *et al.* 1992, Philippot & Van Roermund 1992). Available data on the rheological properties of diopside (Kirby & Kronenberg 1984) would indicate, if the extrapolation is correct, rather high creep resistance at the P–T conditions of eclogitic metamorphism. The contrasting deformation behaviour of clinopyroxene I, which deforms mainly by cataclasis, and diopside-rich clinopyroxene II, which dynamically recrystallizes, may be explained by the difference in chemical composition or by the occurrence of hydrolitic weakening (Champness *et al.* 1974, Buatier *et al.* 1991). Dynamic recrystallization of vein clinopyroxene II, which contains abundant fluid inclusions, to fine-grained fluid inclusion-free aggregates contributes to the hydration of grain boundaries of both vein and adjacent rock and favours the localization of deformation in the shear zone.

The close association of veins and high-strain zones has been recognized in different geological settings over a wide range of pressure–temperature conditions, from low-grade (Segall & Simpson 1983, 1986, Kronenberg *et al.* 1990), to greenschist- and amphibolite-facies (Gibson 1990, Andersen *et al.* 1991, Tobisch *et al.* 1991) and to high-pressure metamorphism (Scambelluri *et al.* 1991, Boundy *et al.* 1992, Früh-Green 1994). This clearly supports the idea that precursor brittle episodes play a fundamental role under a wide range of conditions as a mechanism for nucleating shear zones and deformation partitioning, especially in coarse-grained rocks and rocks with large fractions of strong phases. These rocks exhibit high creep resistance and deform brittlely at the onset of deformation.

Fluids and microfracturing

Grain-scale fracturing is often an important deformation mechanism in mylonites derived from polymineralic rocks, in the presence of high strength contrasts between mineral components. This is well known for deformation of granitoids under medium-grade metamorphic conditions, where dynamic recrystallization of quartz is associated with fracturing of feldspar (e.g. Stünitz & Fitz Gerald 1993 and references therein), at least in the first stage of deformation. In the studied granulites, the macroscopic ductile behaviour under eclogitic conditions is due to the plastic flow of matrix aggregates, largely derived from plagioclase and hornblende sites, in combination with cataclastic deformation of garnet I and clinopyroxene I. During deformation, fluids not only accelerate the crystal–plastic processes in the fine-grained matrix, but also promote brittle deformation of strong phases. The presence of fluids along microfractures is demonstrated by the occurrence of trails of fluid inclusions. Fracturing may be greatly facilitated by fluids due to two reasons.

(1) High P_{H_2O}, which reduces the effective confining pressure (Paterson 1978) and fracture strength of strong mineral phases. Chaotic networks of microfractures in garnet I cores are suggestive of hydrofracturing and $P_{fluid} \geq \sigma_3$ (minimum compressive stress). Partitioning of fluid-pressure and transient high pore fluid pressures may be generated on a local scale by fluctuations of porosity in the embedding ductile matrix, owing to sealing of pore space in matrix aggregates by precipitation from the intergranular fluid and/or crystal plasticity (Fyfe *et al.* 1978, Etheridge *et al.* 1983).

(2) Subcritical crack propagation is possible in the

presence of aqueous fluids by chemical effects at crack tips (stress corrosion) (Atkinson 1982).

Fluid motion and diffusive solute migration may occur in these rocks, in the presence of a segmented fluid film partially wetting the grain boundaries, by a migrating permeability model. The instantaneous configuration of matrix microdomains of low-fluid-interconnectivity is continuously reset during plastic deformation of the fine-grained matrix, through sealing off and opening of pore space, and by communication through transgranular fractures. The dynamic evolution of fluid pathways assists short range mass transfer and fluid flow driven by compositional and pore pressure heterogeneities between contiguous microdomains. Local disequilibrium is clearly indicated by the heterogeneous composition of mineral infilling of cracks. Local scale components of fluid motion and chemical migration may result in a net bulk fluid flow and diffusion towards (and/or away from) large fractures. In this model, the rock permeability is highly dependent on concurrent deformation of the rock.

The close spatial relationship between fractures and mineral re-equilibration of garnet I and clinopyroxene I clearly indicates that fluid access was essential in promoting chemical reactions. Thus, the extent of re-equilibration of garnet I and clinopyroxene I is controlled by the intensity of cataclastic deformation, which to a first approximation increases with increasing bulk deformation. However, the coexistence in the same strain domain of different stages of clast crushing indicates that fracture density is also greatly controlled by small-scale heterogeneities in P_{fluids} owing to episodic low connectivity of fluid pathways. Because of enhanced diffusion via aqueous solutions, rather than slow volume diffusion, the progress of reaction depends strongly on the (hydrated) surface/volume, which is increased by fracturing. In the absence of intragranular fractures, reactions are limited to the external rim along wet grain boundaries, and cores perfectly preserve the original composition. New reaction surfaces are activated along throughgoing fluid-filled cracks. These cracks constitute high-diffusion channels for the introduction and leaching of chemical elements and assist re-equilibration of clasts. Extensive replacement of coarse-grained relics results in the case of pervasive microfracturing. The change in composition of the fracture walls may be factored in two components: (a) a dissolution–precipitation process by interaction between clast and fluid; and (b) solid-state diffusion. These processes may be accelerated by the occurrence of high dislocation densities at the fracture walls, which are often observed around intracrystalline microcracks (White 1975, Smith 1979). Once the fracture has formed, the nature of mineral infilling is determined by the rate of dilatancy. For slow dilatancy rates and low fluid/rock ratios, chemical reaction is buffered by the clast composition (e.g. garnet II bands in garnet I), whereas at high dilatancy rates the mineral infilling is externally buffered (amphibole, omphacite-filled microcracks in garnet I).

CONCLUSIONS

Mesoscale and textural observations demonstrate a close interplay between fluids, deformation and metamorphism during the eclogitization of granulites, which may be summarized as follows.

(1) An increase in flow rate, resulting from grain-size reduction, is allowed or enhanced in the presence of aqueous pore fluids. The degree of reaction softening during replacement of coarse-grained mineral phases by fine-grained aggregates is controlled by the type of synkinematic reactions. The effect is maximized when H_2O-producing reactions occur. Dehydration reactions may to some degree counteract and even overwhelm the effect of grain-size softening.

(2) Hydration gradients can result during brittle episodes either by infiltration of fluids from outside the system along fractures or by re-distribution of internal fluids. The heterogeneity in fluid content is probably the cause of varying rheological behaviour and for deformation partitioning. The opening of veins also results in compositional gradients, due to the different solubility of chemical elements, which contributes to a secondary rheological heterogeneity.

(3) Fluid pressure favours grain-scale fracturing of hard metastable phases, thus contributing to grain-size reduction of the rock. Progressive grain-size reduction of relics affects the bulk deformation by increasing the matrix fraction and by modifying flow patterns. Furthermore, microfracturing increases the reaction surface and the extent of metamorphic re-equilibration owing to the enhancement of reaction kinetics by fluids.

Acknowledgements—This work was supported by grants from CNR and M.U.R.S.T. 40% (S. Martin). Critical reviews by B. Cesare, G. V. Dal Piaz, N. Mancktelow, M. Scambelluri and two anonymous referees substantially improved the manuscript and are gratefully acknowledged. P. Philippot is thanked for discussion, B. Messiga for the SEM facilities and constructive advice, C. Brogiato for photography and A. Novello for thin sections.

REFERENCES

Andersen, T., Austrheim, H. & Burke, E. A. J. 1991. Fluid-induced retrogression of granulites in the Bergen Arcs, Caledonides of W. Norway: Fluid inclusion evidence from amphibolite-facies shear zones. *Lithos* **27**, 29–42.

Atkinson, B. K. 1982. Subcritical crack propagation in rocks: theory, experimental results and applications. *J. Struct. Geol.* **4**, 41–56.

Austrheim, H. 1987. Eclogitization of lower crustal granulites by fluid migration through shear zones. *Earth Planet. Sci. Lett.* **81**, 221–232.

Ballèvre, M., Kienast, J.-R. & Vuichard, J.-P. 1986. La "nappe de la Dent-Blanche" (Alpes occidentales): Deux unités austroalpines indépendantes. *Eclogae geol. Helv.* **79**, 57–74.

Bearth, P., Dal Piaz, G. V., Elter, G., Gosso, G., Martinotti, G. & Nervo, R. 1980. Il lembo di ricoprimento del Monte Emilius, Dent Blanche s.l. — Osservazioni preliminari. *Atti Acc. Sc. Torino* **114**, 227–241.

Benciolini, L. 1989. Evoluzione tettonico-metamorfica del corpo ultramafico di Arpisson (Lembo Austroalpino del Mt. Emilius, Alpi Occidentali). Unpublished Ph. D thesis, University of Padova.

Boundy, T. M., Fountain, D. M. & Austrheim, H. 1992. Structural development and petrofabric of eclogite facies shear zones, Bergen Arcs, western Norway: implications for deep crustal deformation processes. *J. metamorph. Geol.* **10**, 127–146.

Brodie, K. H. & Rutter, E. H. 1985. On the relationship between

deformation and metamorphism, with special reference to the behaviour of basic rocks. In: *Metamorphic Reactions. Kinetics, Textures and Deformation. Advances in Physical Geochemistry*, Vol. 4 (edited by Thompson, A. B. & Rubie, D. C.). Springer, New York, 138–179.

Buatier, M., Van Roermund, H. L. M., Drury, M. R. & Lardeaux, J. M. 1991. Deformation and recrystallization mechanisms in naturally deformed omphacites from the Sesia-Lanzo zone; geophysical consequences. *Tectonophysics* **195**, 11–27.

Champness, P. E., Fyfe, W. S. & Lorimer, G. W. 1974. Dislocations and voids in pyroxene from a low temperature eclogite: mechanism of eclogite formation. *Contr. Miner. Petrol.* **43**, 91–98.

Compagnoni, R., Dal Piaz, G. V., Hunziker, J. C., Gosso, G., Lombardo, B. & Williams, P. F. 1977. The Sesia-Lanzo Zone, a slice of continental crust with high-pressure–low-temperature assemblages in the Western Italian Alps. *Rend. Soc. It. Miner. Petrol.* **33**, 281–334.

Dal Piaz, G. V. 1993. Evolution of Austroalpine and upper Penninic basement in the northwestern Alps from Variscan convergence to post-Variscan extension. In: *Pre-Mesozoic Geology in the Alps* (edited by von Raumer, J. & Neubauer, F.). Springer, Berlin, 327–344.

Dal Piaz, G. V., Lombardo, B. & Gosso, G. 1983. Metamorphic evolution of the Mt Emilius Klippe, Dent Blanche nappe, Western Alps. *Am. J. Sci.* **283**, 438–458.

Dal Piaz, G. V., Gosso, G., Pennacchioni, G. & Spalla, M. I. 1993. Geology of Eclogites and Related Rocks in the Alps. In: *Italian Eclogites and Related Rocks* (edited by Morten, L.). *Acc. Naz. Sci. Roma* **13**, 17–58.

Droop, G. T. R., Lombardo, B. & Pognante, U. 1990. Formation and distribution of eclogite facies rocks in the Alps. In: *Eclogite Facies Rocks* (edited by Carswell, D. A.). Blackie, Glasgow, 225–259.

Durney, D. W. & Ramsay, J. G. 1973. Incremental strains measured by syntectonic crystal growth. In: *Gravity and Tectonics* (edited by De Jong, K. A. & Scholten, R.). Wiley, New York, 67–96.

Etheridge, M. A., Wall, V. J. & Vernon, R. H. 1983. The role of the fluid phase during regional metamorphism and deformation. *J. metamorph. Geol.* **1**, 205–226.

Früh-Green, G. L. 1994. Interdependence of deformation, fluid infiltration and reaction progress recorded in eclogitic metagranitoids (Sesia Zone, Western Alps). *J. metamorph. Geol.* **12**, 327–343.

Fyfe, W. S., Price, N. J. & Thompson, A. B. 1978. *Fluids in the Earth's Crust*. Elsevier, New York.

Gibson, R. G. 1990. Nucleation and growth of retrograde shear zones: an example from the Needle Mountains, Colorado, U.S.A. *J. Struct. Geol.* **12**, 339–350.

Gifkins, R. C. 1976. Grain boundary sliding and its accommodation during creep and superplasticity. *Metall. Trans.* **7**, 1225–1232.

Hudleston, P. J. 1989. The association of folds and veins in shear zones. *J. Struct. Geol.* **11**, 949–957.

Hy, C. 1984. Metamorphisme polyphase et évolution tectonique dans la croûte continentale éclogitisée: les séries granitiques et pelitiques du Mont Mucrone (zone Sesia-Lanzo, Alpes Italiennes). Unpublished thése 3eme Cycle, Université de Paris VI.

Ildefonse, B. & Mancktelow, N. S. 1993. Deformation around rigid particles: the influence of slip at the particle/matrix interface. *Tectonophysics* **221**, 345–359.

Kirby, S. H. & Kronenberg, A. K. 1984. Deformation of clinopyroxenite: evidence for a transition in flow mechanisms and semibrittle behaviour. *J. geophys Res.* **89**, 3177–3192.

Kronenberg, A. K., Segall, P. & Wolf, G. H. 1990. Hydrolytic weakening and penetrative deformation within a natural shear zone. *Am. Geophys. Un. Monogr. Ser.* **56**, 21–36.

McClay, K. R. 1977. Pressure solution and Coble creep in rocks and minerals: a review. *J. geol. Soc. Lond.* **134**: 57–70.

Paterson, M. S. 1978. *Experimental Rock Deformation: The Brittle Field*. Springer, Berlin.

Pennacchioni, G. 1991. Evoluzione strutturale del M. Emilius (Austroalpino, Alpi occidentali). *Rend. Soc. Geol. It.* **14**, 97–100.

Pennacchioni, G., Philippot, P. & Scambelluri, M. 1993. Channellized aqueous fluids controlling eclogitization of granulitic protoliths from the Mt. Emilius Austroalpine unit (Western Alps). *Terra Abs.* (Suppl. to *Terra Nova* **5**) **4**, 19.

Philippot, P. 1987. "Crack seal" vein geometry in eclogitic rocks. *Geodin. Acta* **1**, 171–181.

Philippot, P. & Van Roermund, L. M. 1992. Deformation processes in eclogitic rocks: evidence for the rheological delamination of the oceanic crust in deeper levels of subduction zones. *J. Struct. Geol.* **14**, 1059–1077.

Ramsay, J. G. 1967. *Folding and Fracturing of Rocks*. McGraw-Hill, New York.

Ramsay, J. G. 1980. The crack-seal mechanism of rock deformation. *Nature* **284**, 135–139.

Rubie, D. C. 1983. Reaction enhanced ductility: The role of solid–solid univariant reactions in deformation of the crust and mantle. *Tectonophysics* **96**, 331–352.

Rubie, D. C. 1986. The catalysis of mineral reactions by water and restrictions on the presence of aqueous fluid during metamorphism. *Mineral. Mag.* **50**, 399–415.

Rutter, E. H. 1972. The influence of interstitial water on the rheological behaviour of calcite rocks. *Tectonophysics*, **14**, 13–33.

Scambelluri, M., Hoogerduijn Strating, E. H., Piccardo, G. B., Vissers, R. L. M. & Rampone, E. 1991. Alpine olivine and titanclinohumite-bearing assemblages in the Erro-Tobbio peridotite (Voltri Massif, northwest Italy). *J. metamorph. Geol.* **9**, 79–91.

Segall, P. & Pollard, D. D. 1983. Nucleation and growth of strike-slip faults in granite. *J. geophys. Res.* **88**, 555–568.

Segall, P. & Simpson, C. 1986. Nucleation of ductile shear zones on dilatant fractures. *Geology* **14**, 56–59.

Shea, W. T. & Kronenberg, A. K. 1993. Strength and anisotropy of foliated rocks with varied mica contents. *J. Struct. Geol.* **15**, 1097–1121.

Sibson, R. H. 1981. Fluid flow accompanying faulting: Field evidence and models. In: *Earthquakes Prediction: An International Review* (edited by Simpson, D. W. & Richards, P. G.). *Am. Geophys. Un., Maurice Ewing Ser.* **4**, 593–603.

Smith, E. 1979. Dislocation and cracks. In: *Dislocation in Solids* (edited by Nabarro, F. N. R.). North-Holland, New York, 363–448.

Stünitz, H. & Fitz Gerald, J. D. 1993. Deformation of granitoids at low metamorphic grade. II: Granular flow in albite-rich mylonites. *Tectonophysics* **221**, 299–324.

Thompson, A. B. & Rubie, D. C. 1985. *Metamorphic Reactions. Kinetics, Textures and Deformation. Advances in Physical Geochemistry*, Vol. 4. Springer, New York.

Tobisch, O. T., Barton, M. D., Vernon, R. H. & Paterson, S. R. 1991. Fluid-enhanced deformation: transformation of granitoids to banded mylonites, western Sierra Nevada, California, and southeastern Australia. *J. Struct. Geol.* **13**, 1137–1156.

Van Den Driessche, J. & Brun, J. P. 1987. Rolling structures at large shear strain. *J. Struct. Geol.* **9**, 47–67.

Watkinson, A. J. & Cobbold, P. R. 1981. Axial directions of folds in rocks with linear/planar fabrics. *J. Struct. Geol.* **3**, 211–217.

White, S. H. 1975. Tectonic deformation and recrystallization of oligoclase. *Contr. Miner. Petrol.* **50**, 287–304.

White, S. H. 1976. The effect of strain on the microstructure, fabrics and deformation mechanisms in quartzites. *Phil. Trans. R. Soc. Lond.* **A238**, 69–86.

White, S. H., Burrows, S. E., Carreras, J., Shaw, N. D. & Humphreys, F. J. 1980. On mylonite in ductile shear zones. *J. Struct. Geol.* **2**, 175–187.

Yund, R. A., Smith, B. M. & Tullis, J. 1981. Dislocation-assisted diffusion of oxygen in albite. *Phys. Chem. Miner.* **7**, 185–189.

Yund, R. A. & Tullis, J. 1980. The effect of water, pressure, and strain on Al/Si order–disorder kinetics in feldspar. *Contr. Miner. Petrol.* **72**, 297–302.